ULTRASOUND SPECTROSCOPY

S. R. Aylward[⋆]*, M. McCormick*[⋆]*, H. J. Kang*[⋆]*, S. Razzaque*[†]*, R. Kwitt*[‡]*, M. Niethammer*[◦]

[⋆]Kitware, Inc., North Carolina, USA
[†]InnerOptic, Inc., North Carolina, USA
[‡]University of Salzburg, Austria
[◦]The University of North Carolina at Chapel Hill, USA

ABSTRACT

We introduce the concept of "Ultrasound Spectroscopy". The premise of ultrasound spectroscopy is that by acquiring ultrasound RF data at multiple power and frequency settings, a rich set of features can be extracted from that RF data and used to characterize the underlying tissues. This is beneficial for a variety of problems, such as accurate tissue classification, application-specific image generation, and numerous other quantitative tasks. These capabilities are particularly relevant to point-of-care ultrasound (POCUS) applications, where operator experience with ultrasound may be limited. Instead of displaying B-mode images, a POCUS application using ultrasound spectroscopy can, for example, automatically detect internal abdominal bleeding. In this paper, we present *ex vivo* tissue phantom studies to demonstrate the accuracy of ultrasound spectroscopy over previous approaches. Our studies suggest that ultrasound spectroscopy provides exceptional accuracy and informative features for classifying blood versus other tissues across image locations and body habitus.

***Index Terms*—** Ultrasound, Tissue Classification, Segmentation, Radiofrequency, Trauma, Point-of-Care

1. INTRODUCTION

"Ultrasound Spectroscopy" is introduced as the process of acquiring ultrasound data at multiple power and frequency settings to create a rich description of the underlying materials. We show that ultrasound spectroscopy can be used to form segmented anatomic images, eliminating the need to display and interpret traditional B-mode images and potentially improving the anatomic detail that can be revealed via ultrasound.

Our work is motivated by the growing availability of low-cost ultrasound probes that have the potential to revolutionize patient care in the home, in primary care offices, at the scene of accidents, during patient transport, and throughout hospitals. Point-of-care ultrasound (POCUS) applications include assessing liver cirrhosis and spine scoliosis, detecting the presence of life threatening intra-abdominal bleeding, and reporting optic nerve sheath thickness as an indicator of traumatic brain injury.

Traditionally, ultrasound provides images of anatomy and pathology as (2D and 3D) B-mode images that require significant expertise for interpretation, e.g., a basic understanding of ultrasound physics and hands-on training with an expert to learn how to distinguish inherent ultrasound "noise" from organ boundaries. Even within medical facilities, ultrasound imaging expertise is often limited to ultrasonographers and other dedicated professionals. Until the challenges associated with ultrasound image interpretation can be addressed, the potential of low-cost ultrasound systems cannot be achieved. Ultrasound spectroscopy has the potential to overcome those challenges.

Extensive prior work has been dedicated to the analysis of the RF data that underlies B-mode image generation in an effort to automate ultrasound-based tissue identification [1, 2, 3]. Those researchers have investigated a range of feature sets, speckle reduction methods, and other filtering methods for characterizing that RF data in the hope of developing segmented anatomic images. Those prior efforts, however, have failed to take full advantage of the imaging capabilities of ultrasound probes; they only considered RF data acquired using a single transmission power and frequency setting, and that power and frequency setting was typically chosen based on B-mode appearance, e.g., to balance depth of penetration with anatomic contrast and detail on the B-mode presentation.

By using features from the returned RF signals from multiple power and frequency settings, ultrasound spectroscopy forms a rich representation of the tissues present at each imaged point. The range of tissue subtleties that can be distinguished by our system is beyond the scope of this initial publication. In this paper, we focus on coupling ultrasound spectroscopy with machine learning for the automated detection of pooled blood, e.g., detecting or ruling out intra-abdominal bleeding as part of patient triage at the scene of a car accident, when blunt abdominal trauma is suspected.

Trauma is the leading cause of death among persons ages 1 to 44, and it is estimated that 50-75% of trauma involves abdominal trauma[4]. In abdominal trauma, physical exami-

nation findings for abdominal injuries and concealed hemorrhage are notoriously unreliable and may result in increases in morbidity and mortality[5]. These challenges are particularly prevalent in rural environments where distance from trauma centers means that EMS personnel, with limited equipment and no significant ultrasound training, are primarily responsible for care during the critical "golden hour" after an injury.

In the following section we introduce the methods of ultrasound spectroscopy and its application to tissue / blood classification. In the subsequent section we present results from experiments involving two *ex vivo* tissue phantoms. Those two phantoms are used to simulate different body habitus and anatomic locations. Those experiments demonstrate ultrasound spectroscopy's improved performance compared to traditional approaches. We conclude by discussing several other potential applications for ultrasound spectroscopy.

2. METHODS

For the experiments presented in this paper, we acquired the ultrasound data using the *Interson SeeMore* general purpose abdominal probe. That probe costs $1200. It is controlled and returns data via a USB connection. We have developed Mac, Linux, and Android drivers for it. Our drivers support rapidly changing the power and frequency settings of the probe. The probe consists of a single crystal transducer that is moved within an arc within the curved shell of the ultrasound tip. This general purpose probe can be driven at 15% to 30% of its maximum power to produce high contrast images that are not saturated. The probe can be set to center its transmission frequencies at 2.5, 3.5, or 5.0 MHz.

The steps of ultrasound spectroscopy are as follows:

1. *Planar Reflector Normalization* [6] is used to obtain system-independent RF data, commonly referred to as "quantitative ultrasound" data. This enables our classification system to operate across different ultrasound probes. For our experiments, we devised and imaged a container of 50% canola oil and 50% water, which naturally separate and thereby form an excellent planar reflector. We computed the normalization function for the probe once, prior to all experimentation.

2. *Multi-power and multi-frequency RF data collection*: Via rigid mounts, data can be acquired at multiple power and frequency settings. However, if a probe is to be operated freehand, acquisition frame rates must be considered. The Interson probe provides twelve sweeps (i.e., frames) per second (FPS) at a single power/frequency setting, and if three different power/frequency settings are rapidly alternated and combined to create a single multi-power/frequency scan, then the effective acquisition rate drops to approximately three FPS. Clinical ultrasound systems can achieve over 120 FPS, potentially providing RF data at 10 to 20 different power and frequency settings while still supporting the imaging of dynamic processes. Factor analysis methods such as minimum-redundancy-maximum-relevance (mRMR) or Hilbert-Schmidt Independence Criterion Lasso (HSIC Lasso) algorithms can be used to identify the power and frequency combinations that provide the most useful set of features for a particular classification problem, e.g., distinguishing blood from tissues.

3. *Computing RF features*: Given multiple power and frequency RF signals per frame, we fit Legrende and Chebyshev polynomials to each returned RF signal and use those polynomials' coefficients as features, in addition to using traditional RF signal features such as slope (S), intercept (I), and backscatter (BS) coefficients [6]. Polynomial fitting is accomplished using Python and ITK[1], and those libraries contain a variety of other signal feature extraction methods that could be used to characterize the RF signals, e.g., fractal dimension measures.

4. *Machine learning for classification*: A random forest classifier (as implemented in scikit-learn[2]) is then used to classify the feature vectors. Not shown in the results presented in this paper, we evaluated 10+ classification methods, and random forests outperformed all others.

3. EXPERIMENTS AND RESULTS

Two *ex vivo* tissue phantoms were used to compare variations on ultrasound spectroscopy with traditional approaches to ultrasound-based tissue labeling. The first phantom was used to generate training data only. The phantom consisted of (top to bottom) layers of bovine steak, bovine liver, sheep blood, and bovine steak. The second phantom was only used to generate testing data, it did not contain any bovine liver, see Fig. 1. This second phantom simulated encountering a body location / habitus that was not included during training, and thereby provides a measure of the insensitivity of the classification system to changes in the thickness and type of intervening tissues for blood detection.

Ultrasound spectroscopy data was collected at two different power settings (15% and 30%) and three different frequency settings (2.5, 3.5, and 5.0 MHz). We computed the linear reflector normalization for the probe, and then at each of the six different settings, we recorded and normalized two scans from the first phantom and a single scan from the second phantom.

Using the B-mode images from each scan, we hand-labeled Steak, Liver, and Blood regions in the scan. For each of the six RF data recordings at each pixel within those labeled regions, we computed 7 Legrende polynomial coefficients, 7 Chebyshev polynomial coefficients, RF data slope, RF data intercept, and RF data backscatter. We also computed B-mode value, but we did not use it as a feature in our ultrasound spectroscopy classifications. This produced

[1] www.itk.org
[2] http://scikit-learn.org/

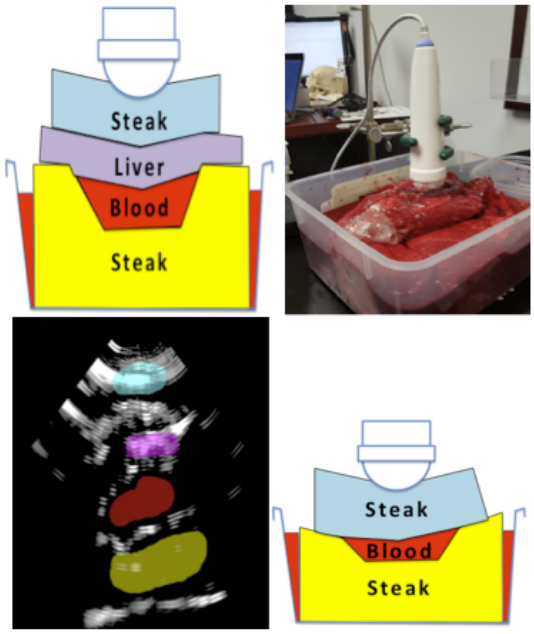

Fig. 1. *Top-Row*: Training images came from a phantom with layers of steak, cow liver, sheep's blood, and steak. *Bottom-Left*: Hand-labeling was used to generate training data from two acquisitions of the training phantom at two different positions, at multiple power and frequency settings. This image shows the hand-labeled classes overlaid on the *Chebyshev Coef 3* feature image from the RF signal at power 15 and frequency 2.5 MHz which greedy feature selection (See Tbl. 2) selected as the most informative for blood-vs-not-blood. *Bottom-Right*: Testing images came from a phantom that did not contain liver - thereby simulating a different imaging location and body habitus.

102 possible ultrasound spectroscopy features at each pixel. Combined with the hand-labeled classes, 10+ classifiers were evaluated, and it was determined that random forest classification produced the best blood-versus-other classification results for most of the sets of features considered.

Results from the various feature sets are given in Table 1. In the first row, the B-mode values from the six different power and frequency settings are used as the feature vector. That produced a true positive rate of only 0.565. In the second and third rows, the 15% power and 2.5 MHz. frequency setting was chosen, since its features were judged to provide the most information in classifying blood-versus-other. At 15/2.5, the use of backscatter, slope, and intercept provided good performance, but the use of all 102 features offered an additional 40% reduction in error. When all features at all frequencies are considered, error drops to 1.51% – nearly an order of magnitude improvement over traditional B-mode interpretation for blood classification.

To gain more insight into the role of multi-frequency and multi-power acquisitions and the role of detailed RF data features such as Legrende and Chebyshev coefficients, we used a greedy feature selection strategy with an information gain metric [7]. That analysis lead to determining the 14 most informative features for blood-versus-other classification, starting from the 102 possible features. The resulting collection of 14 selected features is listed in Table 2. Intersting observations are that (1) every power and frequency setting is represented; (2) nearly every Chebyshev and Legrende coefficient degree is used, albeit from different powers and frequencies; and (3) the traditional features of RF data slope, intercept, and backscatter are not ranked among the top fourteen most informative features, at any power or frequency setting.

Table 1. Four different sets of features were used with random forest classifiers and with two different phantoms, see Fig. 1. There were two powers (15 and 30) and three frequency settings (2.5, 3.5, 5.0 MHz) from which feature sets were either B-mode values; backscatter (BS), slope (S), and intercept (I) of RF signal; or Chebyshev and Legrendre polynomial coefficients along with BS, S, and I. The metrics were the true positive rate (TPR), false positive rate (FPR), and % error for labeling testing pixels as "blood" or "other".

Pwr	Freq	Features	TPR	FPR	%Err
All	All	B-Mode Only	0.565	0.057	13.46
15	2.5	BS, S, I	0.874	0.043	5.99
15	2.5	All	0.921	0.024	3.49
All	All	All	0.948	0.005	1.51

Table 2. Greedy information gain feature selection chose these 14 features for blood-vs-not-blood classification. Ordered by power and frequency.

Pwr	Freq	Feature
15	25	Chebyshev Coef 3
15	35	Chebyshev Coef 4
15	35	Legendre Coef 2
15	35	Legendre Coef 6
15	50	Chebyshev Coef 3
15	50	Chebyshev Coef 5
15	50	Legendre Coef 3
30	25	Chebyshev Coef 4
30	25	Legendre Coef 0
30	25	Legendre Coef 3
30	35	Chebyshev Coef 4
30	35	Legendre Coef 2
30	50	Chebyshev Coef 3
30	50	Legendre Coef 4

4. CONCLUSIONS

Ultrasound spectroscopy involves planar reflector normalization, RF data recordings at multiple powers and frequencies, and features based on approximating the returned RF signals with high degree polynomials. Combined with machine learning methods, it provides a quantitative analysis of anatomy that outperforms previous approaches to ultrasound-based classification of pooled blood versus tissue. Furthermore, the use of multiple powers and frequencies as well as detailed descriptors of the RF signal (e.g., Chebyshev polynomial coefficients) are ranked as the most informative features, compared to traditional RF data features, for blood classification.

Beyond classification, in Fig. 1 we show how generating an image from a single feature can present an alternative view of anatomy that is perhaps easier to interpret than a b-mode image. Future work will explore discriminant analysis methods to determine the linear combination of features that produce images that best distinguish blood from other tissues, that simplify the identification of liver lesions, that enable the assessment of liver cirrhosis, or that improve cross-modality registration accuracy.

Acknowledgements. This work was supported, in part, by NIH R01-CA170665, R44-CA165621, R44-EB016621, and R44NS081792.

5. REFERENCES

[1] J.A. Noble and D. Boukerroui, "Ultrasound image segmentation: a Survey," *IEEE Transactions on Medical Imaging*, vol. 25, no. 8, pp. 987–1010, Aug 2006.

[2] P. Wu, Y. Liu, Y. Li, and B. Liu, "Robust prostate segmentation using intrinsic properties of trus images," *IEEE Transactions on Medical Imaging*, vol. 34, no. 6, pp. 1321–1335, June 2015.

[3] M. Pereyra, N. Dobigeon, H. Batatia, and J. Tourneret, "Segmentation of skin lesions in 2-d and 3-d ultrasound images using a spatially coherent generalized rayleigh mixture model," *IEEE Transactions on Medical Imaging*, vol. 31, no. 8, pp. 1509–1520, Aug 2012.

[4] C. Eskridge, "Trauma Stabilization Services in Rural Texas," *Texas Legislative Council, http://www.tlc.state.tx.us/pubspol/traumaservrural.pdf*, 2004.

[5] E.L. Legome, S.M. Keim, J.P. Salomone, and J. Udeani, "Blunt abdominal trauma," Online at: http://emedicine.medscape.com/article/1980980-overview.

[6] R.J. Lavarello, G. Ghoshal, and M.L. Oelze, "On the estimation of backscatter coefficients using single-element focused transducers," *The Journal of the Acoustical Society of America*, vol. 129, no. 5, 2011.

[7] E. Frank M. Hall, B. Pfahringer G. Holmes, P. Reutemann, and I.H. Witten, "The WEKA Data Mining Software: An Update," *SIGKDD Explorations*, vol. 1, no. 1, 2009.